

RESEARCH

Open Access



Flexible nonlinear modeling reveals age-related differences in resting-state functional brain connectivity in autistic males from childhood to mid-adulthood

Daniel Feldman^{1,2*} , Molly Prigge^{2,3}, Andrew Alexander^{3,4,5}, Brandon Zielinski^{2,6}, Janet Lainhart^{3,4} and Jace King^{1,2*}

Abstract

Background Divergent age-related functional brain connectivity in autism spectrum disorder (ASD) has been observed using resting-state fMRI, although the specific findings are inconsistent across studies. Common statistical regression approaches that fit identical models across functional brain networks may contribute to these inconsistencies. Relationships among functional networks have been reported to follow unique nonlinear developmental trajectories, suggesting the need for flexible modeling. Here we apply generalized additive models (GAMs) to flexibly adapt to distinct network trajectories and simultaneously describe divergent age-related changes from childhood into mid-adulthood in ASD.

Methods 1107 males, aged 5–40, from the ABIDE I & II cross-sectional datasets were analyzed. Functional connectivity was extracted using a network-based template. Connectivity values were harmonized using COMBAT-GAM. Connectivity-age relationships were assessed with thin-plate spline GAMs. Post-hoc analyses defined the age-ranges of divergent aging in ASD.

Results Typically developing (TD) and ASD groups shared 15 brain connections that significantly changed with age (FDR-corrected $p < 0.05$). Network connectivity exhibited diverse nonlinear age-related trajectories across the functional connectome. Comparing ASD and TD groups, default mode to central executive between-network connectivity followed similar nonlinear paths with no group differences. Contrarily, the ASD group had chronic hypoconnectivity throughout default mode-ventral attentional (salience) and default mode-somatomotor aging trajectories. Within-network somatomotor connectivity was similar between groups in childhood but diverged in adolescence with the ASD group showing decreased within-network connectivity. Network connectivity between the somatomotor network and various other functional networks had fully disrupted age-related pathways in ASD compared to TD, displaying significantly different model curvatures and fits.

*Correspondence:

Daniel Feldman
daniel.a.feldman@utah.edu
Jace King
jace.king@hsc.utah.edu

Full list of author information is available at the end of the article



© The Author(s) 2025, corrected publication 2025. **Open Access** This article is licensed under a Creative Commons Attribution-NonCommercial-NoDerivatives 4.0 International License, which permits any non-commercial use, sharing, distribution and reproduction in any medium or format, as long as you give appropriate credit to the original author(s) and the source, provide a link to the Creative Commons licence, and indicate if you modified the licensed material. You do not have permission under this licence to share adapted material derived from this article or parts of it. The images or other third party material in this article are included in the article's Creative Commons licence, unless indicated otherwise in a credit line to the material. If material is not included in the article's Creative Commons licence and your intended use is not permitted by statutory regulation or exceeds the permitted use, you will need to obtain permission directly from the copyright holder. To view a copy of this licence, visit <http://creativecommons.org/licenses/by-nc-nd/4.0/>.

Limitations The present analysis includes only male participants and has a restricted age range, limiting analysis of early development and later life aging, years 40 and beyond. Additionally, our analysis is limited to large-scale network cortical functional parcellation. To parse more specificity of brain region connectivity, a fine-grained functional parcellation including subcortical areas may be warranted.

Conclusion Flexible non-linear modeling minimizes statistical assumptions and allows diagnosis-related brain connections to follow independent data-driven age-related pathways. Using GAMs, we describe complex age-related pathways throughout the human connectome and observe distinct periods of divergence in autism.

Keywords Autism, fMRI, Functional connectivity, Age-related, Cross-sectional, Generalized additive model

Background

Divergent brain connectivity in autism spectrum disorder (ASD) has been extensively studied in humans using resting-state functional magnetic resonance imaging (rs-fMRI) [1–4]. Resting-state fMRI can be used to describe functional brain connectivity, or correlations of between-region brain activity, across brain networks that are associated with various cognitive functions. Previous work has reported widespread patterns of hypo- and hyper-connectivity both within and between these functional networks in ASD [1–4]. Moreover, these functional differences have been shown to relate to symptom severity and symptom profiles in autism. For instance, the degree of default mode network (DMN) hypoconnectivity correlates to social symptom severity in ASD [3]. Likewise, increased local connectivity of the dorsal posterior cingulate cortex (PCC) has been correlated with cognitive inflexibility and behavioral rigidity in ASD [1]. Despite these findings, functional connectivity results and their relationships to cognition have varied, even among modern large-scale mega-analyses, calling into question the reliability and reproducibility of functional connectivity differences in ASD [5–7].

Even more elusive has been understanding the effects of age on brain connectivity trajectories in ASD. Some studies have reported specific default mode network (DMN) within-network hyperconnectivity at a young age which resolved in adolescence to adulthood [8–9]. Another study found childhood DMN, frontoparietal, and salience between-network hyperconnectivity which either persisted into adulthood or decreased to hypoconnectivity in adulthood [10]. These connectivity changes may have been influenced by anatomical distance both within and between networks, with long-range connectivity specifically subject to decreased connectivity with age in ASD [10–11]. However, the specific findings are inconsistent across studies, possibly due to small sample sizes. Indeed, more recent mega-analyses have reported no significant impact of age on divergent connectivity in ASD [5–6].

These inconsistent findings may be due, in part, to the use of varying statistical approaches to relate age and brain connectivity in ASD. Many previous reports have

binning participants into age groupings, such as child (<11), adolescent (11 < 18), and adult (>18), when analyzing brain connectivity changes with age in ASD [8, 10, 11]. However, prior work indicates that developmental connectivity changes occur within these age ranges [12–14]. As such, it may be critical to maintain age as a continuous variable when examining age impacts on brain connectivity.

Beyond age binning, many previous reports have employed linear models to describe brain age-related changes in ASD [5, 6, 15]. However, substantial evidence suggests that some age-related network functional connectivity changes may be nonlinear during typical development (TD) [13, 16–21]. Some prior studies that examined age-related functional connectivity differences in ASD with non-linear analyses limited their modeling to quadratic regression approaches [9, 25, 26]. Polynomial regression studies have reported that TD connectivity-age relationships can vary in polynomial degree based on functional network [19–21]. This diversity in polynomial fit across networks suggests the need for flexible modeling to best describe connectivity-age relationships.

The present study employs generalized additive models (GAMs) to flexibly fit linear and nonlinear typically developing connectivity-age relationships [13, 16, 17]. GAMs are data-driven predictor functions whose curvatures are derived during data fitting [22–24]. As such, GAMs minimize assumptions about data curvature prior to modeling, allowing non-linearities to vary across multiple comparisons. Further, GAMs can resolve data inflection points, allowing identification of developmental periods where participant groups diverge. Here, we revisit the ABIDE datasets considering non-linear, flexible modeling to better describe the relationship between functional connectivity and age in ASD.

Methods

Participants

All 2,226 participants with rs-fMRI imaging included in the ABIDE I & II datasets were initially considered for inclusion in the present analysis. Cross-sectional data from our prior University of Utah longitudinal study (R01MH080826) are included in this dataset. For

site-specific details on both inclusion/exclusion criteria and more detailed characterization of clinical and behavioral phenotypes, see the ABIDE I & II releases [27, 28].

After MRI preprocessing, scrubbing, visual data inspection, and exclusion of sites with fewer than 10 participants (see MRI preprocessing and analysis), 1111 male participants from 25 unique sites remained. Four additional male TD individuals were excluded as statistical age outliers ($z > 4$) to maintain an age-matched dataset. 291 female participants also remained eligible for analysis following data quality control. However, females were not included in the analysis due to disproportionate sex distribution and known sex differences in ASD [29]. Further details on data quality control and participant inclusion are described elsewhere [7].

MRI preprocessing and analysis

Structural MPRAGE data from the ABIDE dataset were processed using FreeSurfer (v6.0.0), which is documented and freely available for download online (<http://surfer.nmr.mgh.harvard.edu/>). Briefly, this processing includes motion correction and averaging [30] of volumetric T1 weighted images, removal of non-brain tissue using a hybrid watershed/surface deformation procedure [31], automated Talairach transformation, segmentation of the subcortical white matter and deep gray matter volumetric structures [32–33], intensity normalization [34], tessellation of the gray matter white matter boundary, automated topology correction [35–36], and surface deformation following intensity gradients to optimally place the gray/white and gray/cerebrospinal fluid borders at the location where the greatest shift in intensity defines the transition to the other tissue class [37–39].

Preprocessing of the ABIDE fMRI blood-oxygen-level-dependent (BOLD) data was performed in MATLAB (MathWorks, Natick, MA, USA) using SPM12 (Wellcome Department of Imaging Neuroscience, London, UK). All images were corrected for motion using a realign and unwarp procedure. Each participant's BOLD images were coregistered to their individual MPRAGE anatomic image sequence. Phase-shifted soft tissue correction (PSTCor) [40] was used to regress participant motion parameters, eroded white matter, eroded cerebral spinal fluid, and soft tissues of the face and calvarium. PSTCor, an alternative to global signal regression (GSR), does not explicitly regress global fMRI signal but rather related signals, as GSR has been shown to artifactually inflate anti-correlations between functional brain networks [40, 41]. Eroded masks were obtained by removing all voxels from white matter and CSF masks that were adjacent to a voxel not in the mask. Volume censoring (scrubbing) was performed with removal of volumes before and after mean framewise displacement head motion greater than 0.3 mm [42]. Only participants with $\geq 50\%$ volumes

remaining after scrubbing were considered for further analysis. Additionally, quality control was completed by J.K. that consisted of visual inspection of each participant's neuroimaging data for successful completion of the preprocessing pipeline and image quality. Individual research sites with less than 10 participants remaining after quality control were removed from further analysis.

Following preprocessing, rs-fMRI images were parcellated using the Yeo et al. 17×17 functional network schema [43]. Functional network connectivity was calculated using the Pearson correlation coefficient between pairs of time series from the parcellated region. This yielded a 17×17 connectivity matrix comprising 136 unique inter-network correlations.

Data harmonization

Connectivity data was then harmonized across sites using ComBat-GAM [44]. ComBat is an empirical Bayesian harmonization technique aimed to mitigate additive and multiplicative site-effects of multicenter neuroimaging data while maintaining biological variability [45, 46]. ComBat traditionally relies on a multiplicative linear regression framework and further assumes a normal distribution of site effects. However, the relationship between brain connectivity and age is presently hypothesized to be non-linear and non-parametric. As such, we implement ComBat-GAM, a generalized additive model ComBat framework that allows preservation of nonlinear covariate effects [44].

Generalized additive models

GAMs, unlike parametric regressions, do not contain a priori specification of predictor relationships [22–24]. Rather, GAM prediction functions are derived during model estimation [22–24]. This process eliminates regression model refinement and predictor selection, which is burdensome and error-prone when analyzing hundreds to thousands of unique models during large connectivity analysis [22].

Thin-plate splines (TPS) are the suggested optimal basis function to enable independent smooth functions of multiple predictors in GAMs [24, 45]. TPS use a penalized least squares method to mitigate over-smoothing while maintaining model flexibility [24, 47]. The final GAM curve is the weighted summation of a series of TPS fits in the data [22–24]. In doing so, GAM relationships can span a spectrum of linearity and non-linearity. Further, GAMs can resolve sharp data inflection points, which are often obscured in polynomial regression.

The GAMs presently used follows the mathematical framework:

$$y = \beta_0 + \sum (\beta_i * x_i) + f(x_1, x_2)$$

Where y is the predicted variable, β_0 is the intercept, β_i is the linear coefficient for the linear predictor variable x_i , and $f(x)$ is the smooth function of predictor variables. The smooth function was defined by the thin-plate spline:

$$\phi(r) = r^2 * \log(r)$$

Where r is the Euclidean distance between a data point and a given knot, following the penalized least squares optimization:

$$\sum (y_i - f(x_i))^2 + \lambda * \iint (\nabla^2 f(x, y))^2 dx dy$$

Where λ is the smoothing parameter and ∇^2 is the Laplacian operator. Taken together, our general additive model follows the equation:

$$\begin{aligned} \text{Brain Connection} \\ \sim \beta_0 + f_1(\text{Age}) + f_2(\text{Age Group}) \\ + \beta_{\text{Group}} * \text{Group} \\ + \beta_{\text{Head Motion}} * \text{Head Motion} + \epsilon \end{aligned}$$

Where $f_1(\text{Age})$ is a TPS of TD age, $f_2(\text{Age, Group})$ is a contrasted TPS of ASD age, $\beta_{\text{Group}} * \text{Group}$ is a predictor of *Group*, and $\beta_{\text{Head Motion}} * \text{Head Motion}$ is treated as a nuisance regressor.

A. Statistical analysis and visualization.

All statistical analyses and visualizations were conducted in R [48] (Version 4.4.1). Data were visualized using the ggplot2 R package [49]. Following harmonization, the relationship between each brain connection and participant age was analyzed using a TPS GAM with a maximum of 10 knots using the R mcgv package [50] (version 1.9.1).

Model significance was defined by age-related variables and was corrected for multiple comparisons using a Benjamini-Hochberg correction. Significance was defined as a connectivity-age relationship with corrected $p < 0.05$. For models in which the TD and ASD functional connectivity development trajectories both significantly changed with age, post-hoc pairwise analysis of the predicted models was used to define age ranges of group differences in aging using the tidy-gam package [51] (version 1.0.7). Specifically, pairwise significant differences were defined as where the 95% confidence interval of the difference between predicted curves was bound above or below 0.

Model evaluation

All significant models were evaluated to ensure the statistical assumptions of our GAM, namely residual

homoscedasticity and residual normal distributions, were not violated. Residual homoscedasticity was assessed by plotting model residuals against predicted values. Residual distribution was visualized with a Q-Q plot and quantified with skewness, kurtosis, and Shapiro-Wilks normality tests.

Model reliability

Model reliability was evaluated with a stratified 5-fold split-sample validation. The mean correlation and standard deviation between the split-sample curve fits and the entire model fits at each year (5–40) were calculated to quantify model similarity. TD and ASD curves were independently analyzed and compared with a two-sample t-test across curve correlations to determine if reliability was group dependent.

Comparison to prior methods

Previous studies have commonly implemented both linear models and age-binning approaches to describe the relationships between functional connectivity, age, and ASD [5, 6, 8, 10, 11, 15]. To compare our model to these previous approaches, we implement both a linear model and age-binned ANCOVA on our harmonized dataset. Ages were binned as < 11 , $11-18$, and > 18 , mirroring previous studies [8, 10, 11]. The linear model followed the equation:

$$\text{Brain Connection} \sim \text{Age} * \text{Group} + \text{Head Motion}$$

while the ANCOVA followed the equation:

$$\text{Brain Connection} \sim \text{Binned_Age} * \text{Group} + \text{Head Motion}$$

where mean motion was treated as a nuisance regressor. P-values for the main effects of group, Age, and their interaction were extracted and Benjamini-Hochberg corrected for 136 comparisons. All statistical analyses were conducted in R [46] (Version 4.4.1).

Replication with Yeo 7 parcellation

Brain parcellation schemas have recently been shown to impact relationships between functional network connectivity and age [52, 53]. To this end, we presently attempted to replicate our findings using the Yeo et al. 7×7 functional network parcellation [43]. Importantly, the Yeo 7×7 schema does not allow for within-network analyses, limiting reproducibility comparisons to between-network analyses. Replication data processing, harmonization, modeling, and analyses follow previously described methods.

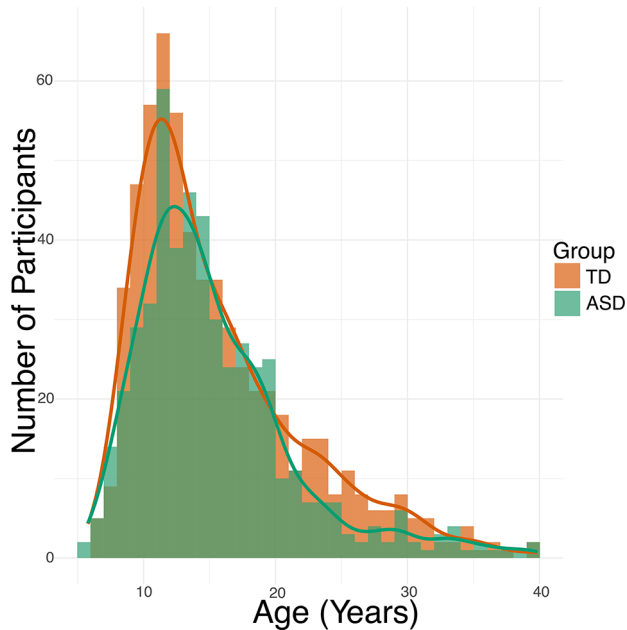


Fig. 1 Participant age range. Bars are a histogram of participant age binned into integer age ranges. Curves are density plots of the age distribution by group

Results

Participant demographics

In the ABIDE I data release, 1112 participants were analyzed and 419 were removed (220 due to motion, 199 due to other quality issues). In the ABIDE II data release, 1114 participants were analyzed and 405 were removed (217 due to motion, 188 due to other quality issues).

After excluding the remaining females and four age outliers ($z > 4$), a total of 1107 age-matched males ranging from 5 to 40 years old ($N[\text{Mean, STD}], \text{TD} = 610[15.18, 6.38], \text{ASD} = 497[14.90, 6.01]$) were included in the final analysis (Fig. 1). Of the final 1107 participants included, $15 \pm 12\%$ of volumes were censored for TD participants and $18 \pm 13\%$ of volumes were censored for ASD participants across sites ($t(1105) = 4.16, p < 0.001, 95\% \text{ CI } [0.02-0.05]$). There was no significant difference in mean age between the groups. Age distribution in both groups followed a positive-skewed Gaussian distribution.

Diverse trajectories of functional brain development

Of the 136 analyzed brain functional connections, 55 changed significantly with age in the TD group ($p\text{-FDR} < 0.05$) (Fig. 2). In the ASD group, 19 functional connections changed significantly with age ($p\text{-FDR} < 0.05$), of which, 15 overlapped with TD. Nine of these 15 connections displayed significantly different connectivity-aging trajectories in ASD compared to TD. Curvature of these connectivity-age trajectories were diverse both between and within networks, highlighting model flexibility enabling analysis of differential age-related pathways throughout brain networks.

Fully disrupted linear age-related pathways in ASD

Post-hoc analyses of overlapping significant trajectories revealed six disrupted age-related pathways in ASD (Fig. 3). These six overlapping FDR-corrected between-network age-related trajectories displayed significantly different model fits and shapes between the ASD and TD

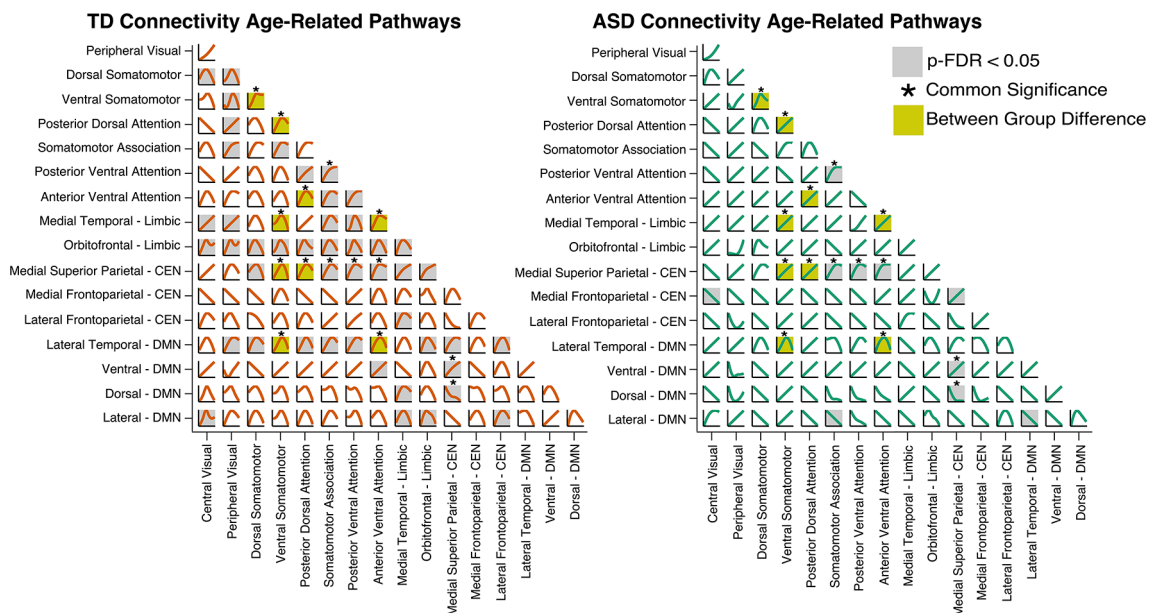


Fig. 2 Trajectories of functional brain development. Each individual curve displays connectivity strength (y-axis) with increasing age (x-axis, range 5–40). Connections that varied significantly with age after multiple comparison corrections are shaded in gray. *Common significant connections shared by both ASD and TD. Significant between group differences highlighted in gold

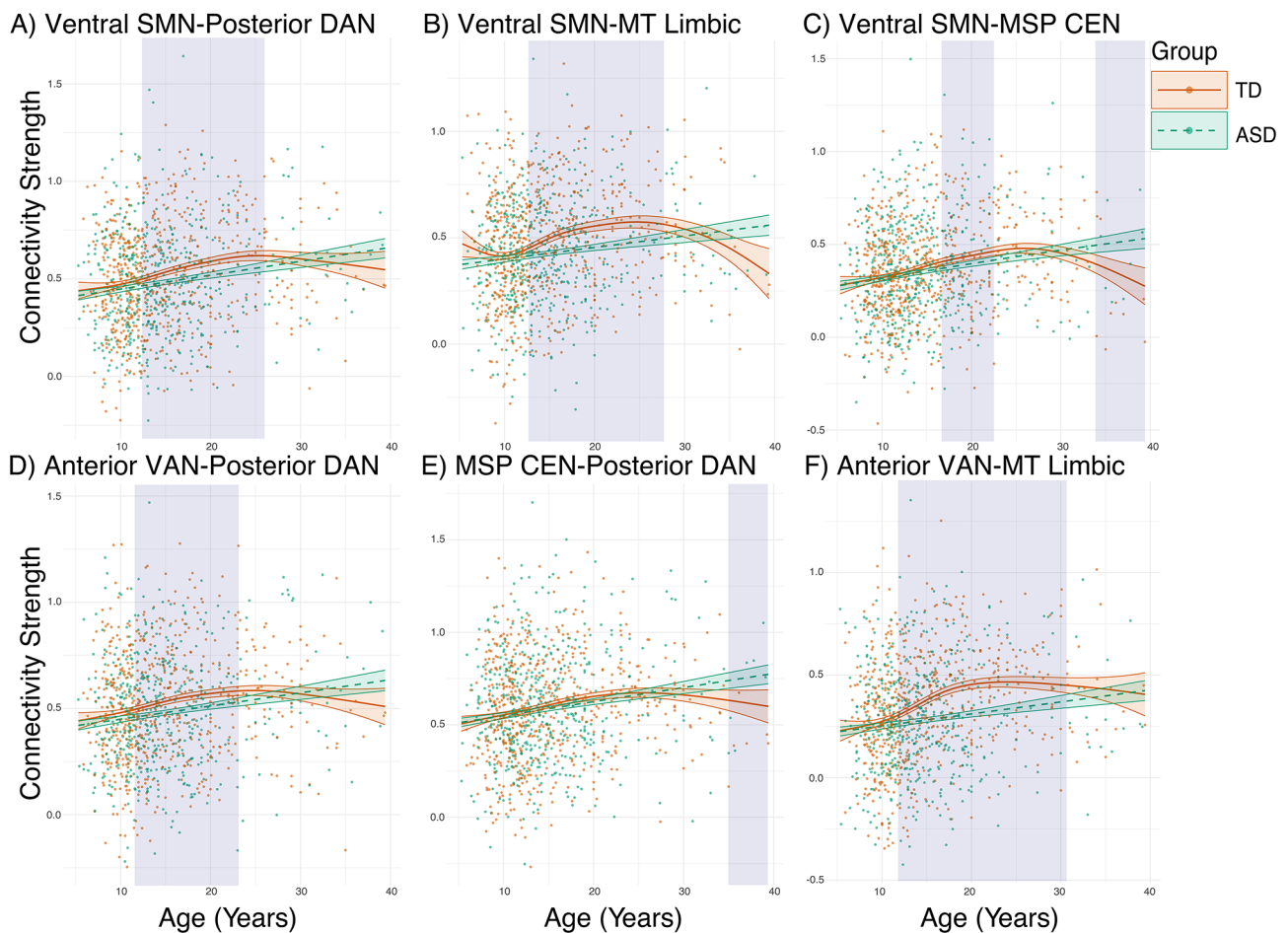


Fig. 3 Fully disrupted linear age-related pathways in ASD. Between-network connections displayed fully disrupted age-related pathways in ASD, demonstrated by entirely different model fits compared to TD. TD between-network SMN development increased in childhood and stabilized or decreased in young adulthood. Contrarily, ASD SMN connectivity was best modeled by an increasing linear model, displaying group-by-age interactions in ASD. Similarly, both the anterior VAN and MSP-CEN had disrupted connectivity-age-related pathways with the posterior DAN. A similar trend was seen in limbic-VAN connectivity. All results are FDR-corrected. Shaded areas denote regions of pairwise differences between groups. Acronyms: somatomotor network (SMN), dorsal attention network (DAN), medial temporal limbic (MT-limbic), medial superior parietal (MSP), ventral attention network (VAN)

groups. In all six models, non-linear age-related changes are seen in the TD group with increases in childhood and adolescence followed by stabilization or decreases in connectivity in adulthood ($p\text{-FDR} < 0.05$). Contrarily, the ASD group connectivity increases linearly with age throughout the analyzed age range ($p\text{-FDR} < 0.05$). These disrupted linear pathways are seen between the somatomotor network (SMN) and the dorsal attention (DAN), limbic, and medial superior parietal central executive (MSP-CEN) networks. Likewise, both the anterior ventral attention (aVAN) and MSP-central executive networks display these disrupted models in their connectivity to posterior dorsal attention (pDAN) network, different from the congruent MSP-central executive to VAN age-related pathways as seen in Fig. 4. Lastly, limbic-aVAN connectivity also displayed a disrupted linear path.

DMN between network chronic underconnectivity in ASD

Between network connectivity of the lateral-temporal DMN and the anterior VAN varied significantly with age in both the ASD and TD group (TD: $p\text{-FDR} < 0.001$; ASD: $p\text{-FDR} = 0.005$) (Fig. 5). Both groups followed an inverse parabolic connectivity-age path. The ASD group had significantly decreased DMN-VAN connectivity that persisted from age 8–26 (pairwise 95% C.I. > 0) and continued non-significantly throughout the analyzed age range. A similar chronic underconnectivity was seen between the lateral-temporal DMN and the ventral SMN (TD: $p\text{-FDR} < 0.001$; ASD: $p\text{-FDR} = 0.004$), with significant hypoconnectivity ranging from ages 5–31 (pairwise 95% C.I. > 0).

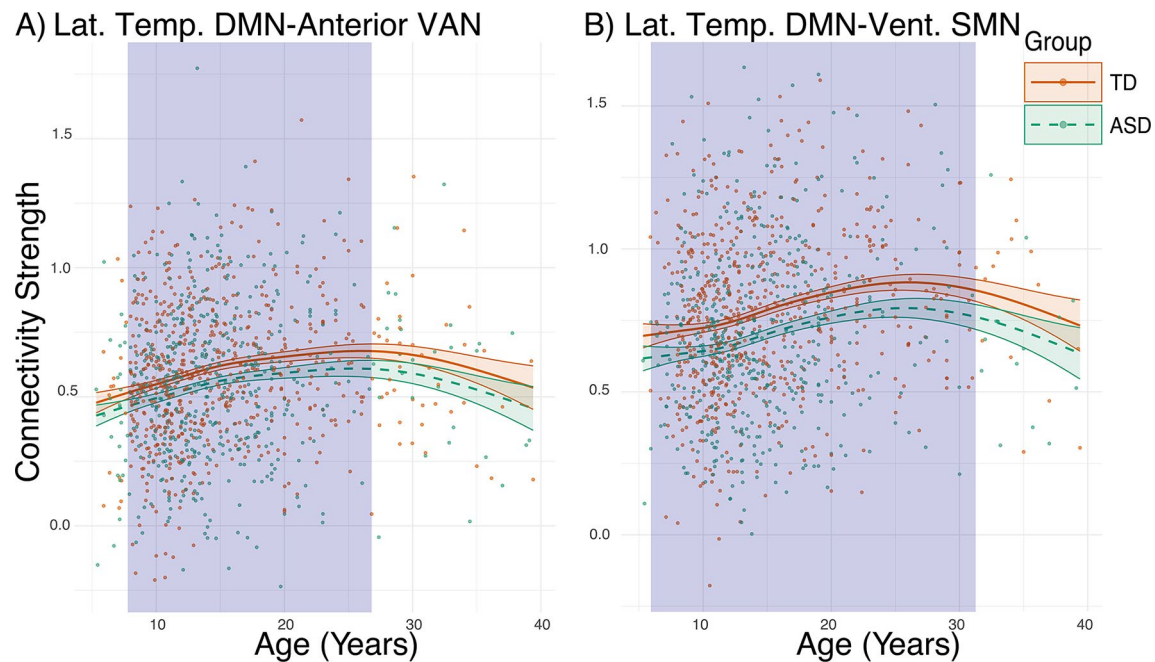


Fig. 4 Default mode between-network chronic underconnectivity in ASD. The lateral temporal DMN subcomponent showed decreased between-network connectivity to both the anterior VAN and somatomotor networks throughout the analyzed period. The general trajectories of the groups followed a similar model curvature. Shaded areas denote regions of pairwise differences between groups. Acronyms: somatomotor network (SMN), ventral attention network (VAN), default mode network (DMN)

Within somatomotor network divergent age-related differences in ASD

Within-network somatomotor connectivity varied significantly with age in both ASD and TD groups (Fig. 6). Both ASD and TD SMN connectivity followed a sinusoidal age-related pathway (TD: $p\text{-FDR} < 0.001$; ASD: $p\text{-FDR} < 0.001$). Connectivity paths between the two groups were similar through childhood but significantly diverged in late adolescence with ASD showing decreased within-network connectivity from ages 18–27. This decreased connectivity trend continued from between ages 27–40, though not statistically significant.

Congruent aging between ASD and TD

Six between-network connections followed congruent age-related paths with no significant group differences between ASD and TD (Fig. 4). In both groups, both connectivity between the ventral and dorsal DMN and MSP-CEN changed significantly with age. Connectivity between the MSP-CEN and ventral DMN increased linearly with age in both TD and ASD groups (TD: $p\text{-FDR} = 0.001$; ASD: $p\text{-FDR} = 0.013$). In contrast, connectivity between MSP-CEN and dorsal DMN decreased in a curvilinear manner throughout the analyzed period (TD: $p\text{-FDR} = 0.005$, ASD: $p\text{-FDR} = 0.004$).

Both subcomponents of the VAN varied significantly with age with the MSP-CEN in both the ASD and TD groups. VAN-CEN connectivity changes with age followed similar pathways for both posterior and anterior

VAN networks, with an increase in childhood that leveled horizontally in early adulthood (CEN-pVAN: TD: $p\text{-FDR} < 0.001$; ASD: $p\text{-FDR} = 0.004$) (CEN-aVAN: TD: $p\text{-FDR} < 0.001$; ASD: $p\text{-FDR} = 0.003$). Lastly, both the MSP-CEN and pVAN networks curvilinearly increased significantly with the somatomotor association (SMNa) network (CEN-SMNa: TD: $p\text{-FDR} < 0.001$; ASD: $p\text{-FDR} = 0.002$) (pVAN-SMNa: TD: $p\text{-FDR} < 0.001$; ASD: $p\text{-FDR} = 0.003$).

Model evaluation

Given the positive-gaussian age skew of our datasets, all models were evaluated for statistical validity. Model evaluations showed that all 15 reported models did not violate the assumptions of residual homoscedasticity. Further, residual distributions all had a Shapiro-Wilks value $W > 0.992$, a kurtosis between 2.922 and 3.305, and a skewness between 0.022 and 0.351. Further, residual distribution did not differ between ASD and TD groups for any significant model (two-sample t-test, $p > 0.05$). Connection-level model evaluations and visualizations can be seen in Supplementary Table 1 and Supplementary Figures S1–S15 [Additional File 1].

Model reliability

A stratified 5-fold split-sample evaluation revealed high levels of curve reproducibility across all significant models. On average, the curve correlation for TD was 0.966 ± 0.024 while the curve correlation was

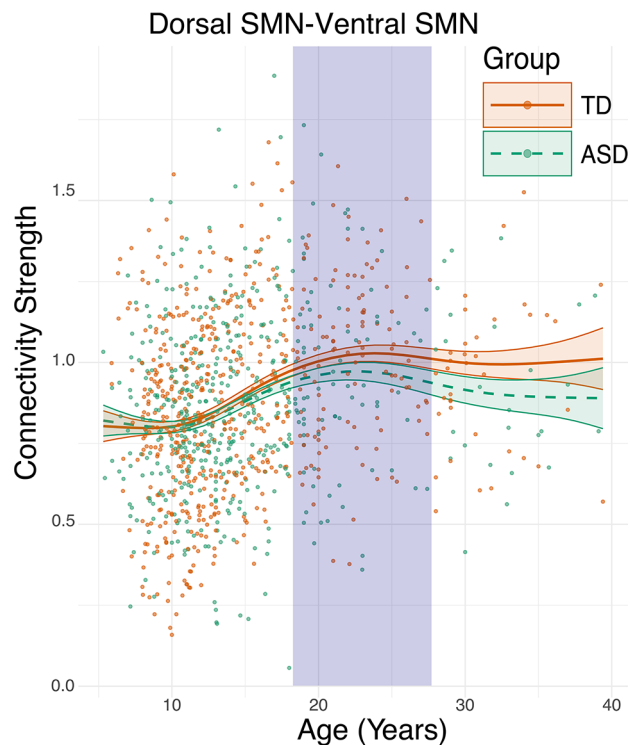


Fig. 5 Within somatomotor network divergent age-related trajectories in ASD. Both ASD and TD within-somatomotor connectivity followed an increasing sinusoidal aging pathway through childhood to mid adolescence. Beginning in late adolescence, the ASD group diverged to sustained hypoconnectivity as the curves horizontally stabilized. Shaded area denotes region of pairwise differences between groups. Acronyms: somatomotor network (SMN)

0.962 ± 0.028 in the ASD group. There were no differences in reliability between ASD and TD groups ($t(28) = 0.779$, $p = 0.442$). Reliability results on the connection-specific level can be seen in Supplementary Table 2 [Additional File 1].

Comparison to prior methods

Linear models analyzing the main effects of age, group, and their interaction yielded 57 brain connections that changed significantly with age, regardless of group (p -corrected < 0.05). No linear model group differences nor model interactions were significant following correction for multiple comparisons.

Binned age ANCOVAs, with ranges < 11 , $11-18$, and > 18 , analyzing age, group, and their interaction yielded 30 brain connections that had a significant effect of binned age (p -corrected < 0.05). Additionally, 47 brain connections had a significant main effect of group (p -corrected < 0.05). However, there were no significant age-by-group interactions following correction for multiple comparisons.

Replication with Yeo 7 parcellation

Brain parcellation schemas may impact relationships between functional network connectivity and age [52, 53]. As such, we report a repeated GAM analysis with the larger-scale Yeo 7-network parcellation schema to examine the reproducibility of between-network findings. Of the 21 analyzed brain functional connections represented in the 7-network parcellation, seven changed significantly with age in the TD group (p -FDR < 0.05). Six of these seven represented connections between the limbic network and all other networks in the brain (visual, SMN, VAN, DAN, CEN, and DMN). Connectivity between these regions and the limbic network non-linearly increased in childhood and adolescence followed by stabilization or decreases in connectivity in adulthood, mirroring the more granular TD between-network limbic connectivity findings reported with the 17-network parcellation. Additionally, VAN-DAN between-network connectivity curvilinearly increased with age in the TD group (p -FDR < 0.05).

No functional brain connections significantly changed with age in the ASD group following statistical correction for multiple comparisons (p -FDR > 0.05). Interestingly, most of these non-significant ASD curve fits were linear, also reflecting increased linearity in ASD compared to TD reported with the 17-network parcellation.

Discussion

Using a flexible GAM framework, we found varying non-linear connectivity-age relationships in typically developing (TD) individuals both within and between functional brain networks. Moreover, we found network-dependent coherence and deviations from these non-linearities in autism spectrum disorder (ASD). Specifically, the ASD group often followed typically developing connectivity-age-related pathways in between-network connectivity to the central executive network (CEN). Contrarily, we found chronic hypo-connectivity of multiple functional networks to the default mode network (DMN). We identified within-network somatomotor (SMN) hypoconnectivity in ASD, which specifically emerged in late adolescence. Lastly, we described fully disrupted age-related pathways in ASD localized to somatomotor, ventral attention (VAN), and limbic networks. ASD and TD coherence and deviations depend on network sub-parcellations. Taken together, our findings highlight the importance of flexible, non-linear modeling to describe divergent age-related trajectories in ASD and describing group differences that may emerge during certain periods of development.

Our findings replicate some from previous literature. Typically developing within-network connectivity has been reported to largely follow inverted U shape aging curves that decline or remain stable beginning

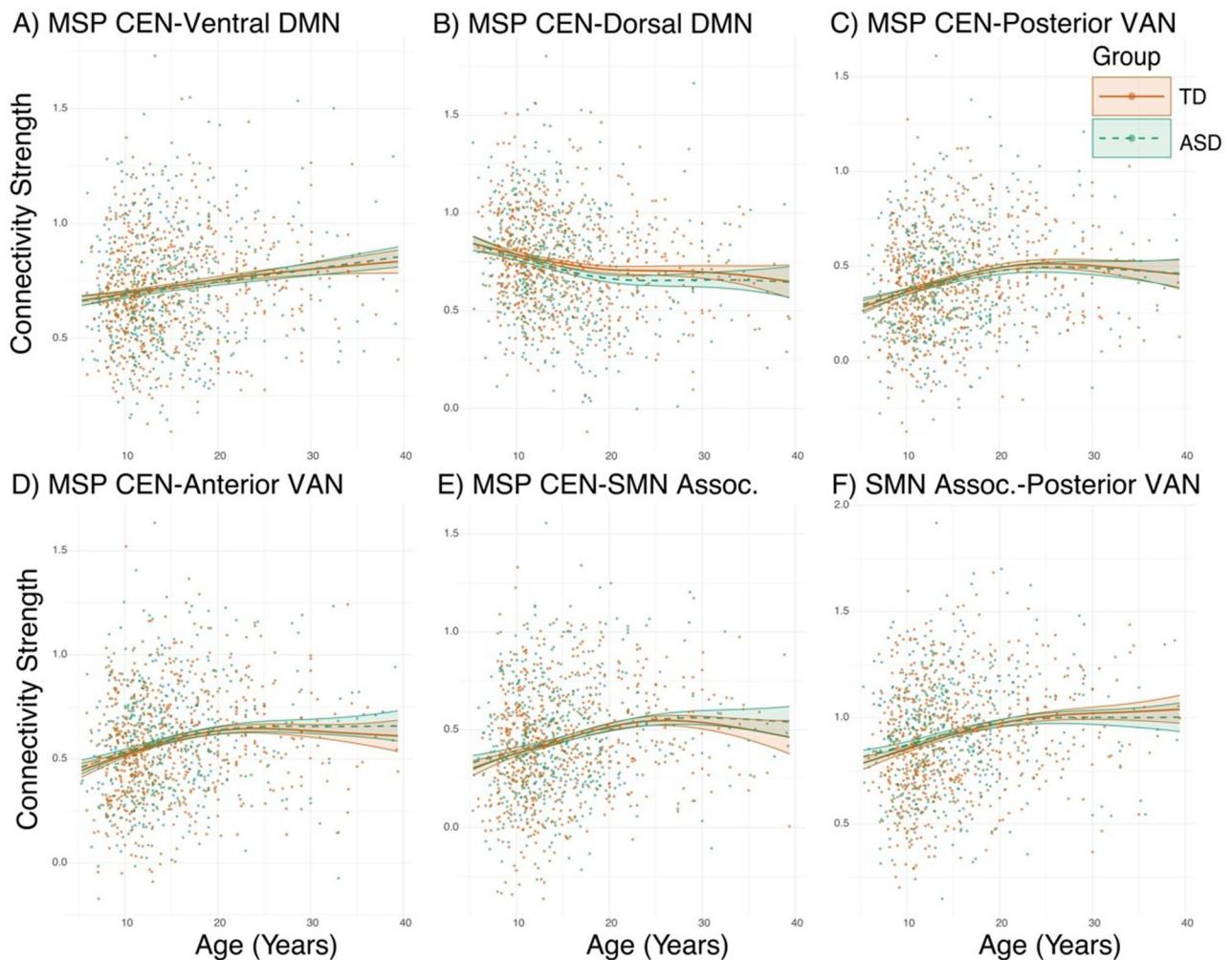


Fig. 6 Congruent age-related group trajectories between ASD and TD. CEN between-network connectivity both increased and decreased depending on separate sub-components of the DMN. MSP-CEN to VAN connectivity increased at a young age and horizontally stabilized beginning in early adulthood. A similar trajectory was seen in CEN-ATTN and SMNa-ATTN connectivity. Acronyms: medial superior parietal central executive network (MSP-CEN), default mode network (DMN), ventral attention network (VAN), somatomotor association network (SMNa)

in late adolescence [16, 18, 19, 21]. We report similar trends with ventral attention, dorsal attention, limbic, and central executive within-network connectivity. We break from previous findings in TD between-network connectivity changes with age. While previous studies have reported initial decreases followed by increases in DMN-CEN and DMN-dorsal attention (DAN) connectivity from childhood to early adolescence in typical development, we report steady increases during this period [16, 18]. These differences may be due to lack of harmonization despite the use of multisite data in these previous studies. Indeed, harmonization has been shown to improve power, sensitivity, and reliability in detecting connectivity-age relationships [54, 55]. Additionally, differences in our findings may be due to different parcellation schemas used in these studies which did not subdivide networks into multiple components as reported in the present study. Despite these differences in

parcellation, our typically developing SMN between-network connectivity results mirror those reported by others, following cubic and sinusoidal curves [16, 17, 20, 21].

While two previous studies examined quadratic regression models of functional connectivity aging in ASD, their second-order polynomial approach may have resulted in limited findings [9, 25]. Indeed, previous reports have found complex non-linear divergent age-related changes in structural brain volume and cortical thickness in ASD [56–58]. Here, we report nonlinear functional connectivity across a multitude of functional networks in ASD. In doing so, we describe congruent and divergent age-related trajectories of functional connectivity in ASD.

DMN between network hypoconnectivity has been reported in numerous previous studies [5, 6, 8, 11, 59]. In line with these reports, we show between-network DMN-VAN and DMN-SMN hypo-connectivity in ASD

that persists from childhood to adulthood. Importantly, the ASD group follows a similar inverse U-shaped aging trajectory in these connections with a constant decreased connectivity. Contrary to previous findings, we also report that age-related trajectories of between-network CEN connectivity with two other subcomponents of the DMN are congruent with TD individuals. These findings suggest that DMN between-network differences in ASD are not universal but may be localized to specific processes within the DMN. Indeed, previous studies of children with ASD have shown hyperconnectivity between the posterior cingulate and temporal cortex compared to TD, with simultaneous hypoconnectivity between the precuneus and visual cortex and basal ganglia [60]. Our results, combined with previous work, suggest between-network DMN differences in ASD may be sub-network specific.

The default mode network is implicated, among other processes, in self-referential thinking, passive sensory processing, and 'theory of mind' -- the ability to infer emotions and mental states of others [61–63]. Common ASD symptomatology includes sensory sensitivity, disruption of sensory integration and processing, and motor deficits [64, 65]. DMN hypo-connectivity to the somatomotor network implies a disconnect between active and passive sensory processing which is potentially relevant to sensory processing differences in ASD. Likewise, chronic DMN hypoconnectivity to the salience network may relate to theory of mind deficits in ASD, as detection of salient external events in reference to internal self-thought would be disrupted [66].

We also report divergent connectivity both within and between somatomotor network subcomponents in ASD. Within SMN connectivity follows a similar sinusoidal path in both ASD and typical development through childhood, but the ASD group departs from this path in adolescence and displays underconnectivity. Two recent mega-analyses reported within-network sensory-motor hypoconnectivity [5, 6]. Further, these hypoconnectivity directly correlated with self-reported sensory deficits and restricted social behavior [5]. While neither study reported age effects on these findings, they also implemented linear models in their analysis. Here, we similarly find within-SMN hypoconnectivity in ASD but report a non-linear aging pathway with hypoconnectivity specifically emerging in adolescence. Further, we find divergent aging of SMN between-network connectivity to the DAN, limbic, and CEN networks in ASD. Cubic-resembling SMN connectivity changes with age in typical development have been previously reported [16, 17, 20, 21]. Our results replicate this finding, while simultaneously revealing a completely divergent positive linear age-related pathway in ASD. As previously noted, common ASD symptomatology includes sensory sensitivity,

disruption of sensory integration and processing, and motor deficits [65, 66]. Disrupted connectivity from the SMN to the DAN and CEN may contribute to decreased multi-sensory integration and sensory filtering, potentially contributing to sensory sensitivities and overstimulation often reported in ASD [67].

Divergent linear age-related pathways in ASD are also evident in between-network connectivity to the DAN. Interestingly, these divergent linear relationships are only present in connection with the posterior DAN containing the middle frontal gyri, supramarginal gyri, extrastriate cortex, and parietal cortex. In contrast, between-network connectivity to the dorsal-attention related somatomotor association network containing the fusiform and angular gyri shows congruent aging to TD. These results, along with DMN parcel dynamics, indicate that network parcellation size and schematics may influence the ability to detect specific brain connections exhibiting divergent age-related trajectories with GAMs. Indeed, prior studies have shown that parcellation schemas may impact relationships between functional network connectivity and age [52, 53].

To this end, we repeated our GAM analyses using a 7-network parcellation, which collapses the network subcomponent in our main analysis into seven large-scale network parcellations: visual, VAN, DAN, SMN, CEN, and DMN [43]. Using this large-scale parcellation, we replicate some TD aging pathways, largely pertaining to between-network limbic connectivity. Likewise, in the 7-network parcellation, the ASD aging paths and ASD-TD group relationships resembled those subsets of fully disrupted pathways described with 17-network framework. However, ASD replications and group differences with the 7-network parcellations failed to reach statistical significance after correction for multiple comparisons.

Our results highlight the need for flexible, non-linear modeling when analyzing the relationship between age and functional connectivity. To further demonstrate this, we repeated common linear model and age-binned ANCOVA analytical approaches to our harmonized 17-network dataset [5, 6, 8, 10, 11, 15]. Linear models revealed 42% of brain connections that changed significantly with age but yielded no significant group differences or group interactions following statistical corrections. Differently, the ANCOVA approach, where ages were binned at <11, 11–18, and >18, yielded fewer significant age-related changes in connectivity but resulted in significant group differences in at least one age bin in 35% of the connections.

These results highlight strengths, pitfalls, and the need for improvement in these common approaches. Linear models examine age as a continuous variable, allowing detection of connectivity changes across the age range, but are rigid and inadaptably to varying group differences

that appear in some age ranges, but not others. Meanwhile, binned ANCOVAs are less powered to detect age-related changes in connectivity, as they compare changes across few binned groups. However, ANCOVAs allow group differences to be parsed during different age ranges, albeit pre-defined bins in which connectivity is known to dynamically change with age [12–14].

Generalized additive models address and improve upon both previous methods by maintaining age as a continuous variable while simultaneously allowing non-linear group differences to be parsed at any age range along the fitted curve. In doing so, GAMs can resolve the timing in which aging curvatures depart. Combined with increased sensitivity to inflection points compared to regression models, GAMs serve to define critical periods of connectivity divergence among groups.

Recent studies of cortical brain aging have employed general additive models for location scale and shape (GAMLSS) to explore brain changes throughout the human lifespan [68–71]. GAMLSS, an extension of GAMs, increases model flexibility by incorporating variance (scale) and distribution (shape) terms [72]. GAMLSS are particularly useful in cases of complex distribution with inhomogeneous variance and have most often been applied to define centiles in normative aging [68–71].

Given that the models currently do not violate residual homoscedasticity and normality assumptions, we currently employ the GAMs, not GAMLSS, for model simplicity and ease of interpretation. Further, the additional parameters in GAMLSS pose challenges with data sparsity, which is present at older ages in the ABIDE sample. In GAMLSS, errors are calculated on both mean and variance functions, which in sparse data can artificially inflate or deflate confidence intervals. For instance, if variance is underestimated due to sparsity, GAMLSS prediction intervals can be misleadingly tight which would lead to false detections of group differences in sparse regions. GAMs, whose errors depend on the mean function alone, are more transparently interpretable in this sparse scenario. It is important to note that GAMs' penalized least squared splines limits model curvature inflection in sparse data, combatting overfitting at the potential loss of detecting small effects. Detection of smaller effects at older ages will be enabled by future data on aging in autism, which we are currently collecting (R01MH132218).

We presently apply GAMs for a conservative, interpretable approach to analyzing aging differences in autism. Nevertheless, GAMLSS and other extended GAM frameworks should be considered when analyzing complex data distributions. Generalized additive model statistical frameworks can be extended to many biological use cases where multiple comparisons are common. GAMs

offer a data-driven modeling approach which minimizes assumptions about unique biological features relationship to a variable of interest. In doing so, GAMs ease the burden of regression model optimization, which is often unrealistic and time consuming when performing hundreds to thousands of models in large biological analyses.

Limitations

The present analysis contains several limitations. First, it is important to study autistic females as well as autistic males as divergent connectivity in ASD has been reported to be sex-dependent [73, 74]; the ABIDE samples did not have a sufficient number of females for our analyses. Second, we analyzed a restricted age range, ranging from childhood to mid-adulthood, thereby not allowing analysis across the full lifespan, including very early childhood and later in life brain aging. Future functional brain aging studies of older autistic adults, one of which is currently underway (R01MH132218), will help in the understanding of the biological bases of aging comorbidities associated with autism, such complex mental and physical health comorbidities which are currently understudied and ill-defined [75, 76]. Third, our analysis is limited to large scale network cortical functional parcellation. Subcortical functional connectivity may be fundamental to understanding aberrant aging in ASD [1, 9, 15]. To parse more specificity of brain region connectivity, a fine-grained functional parcellation including subcortical areas may be warranted. Fourth, post-hoc analyses of fitted curves were not corrected for multiple comparisons within each model. GAMs do not enable multiplicative group interactions as multiple trajectories are fit to different degrees of curvature. As such, between group differences rely on post-hoc comparisons of predicted values, which limits statistical power [72]. Finally, our age-related analyses used the cross-sectional data from ABIDE, rather than longitudinal data. As such, we focused on age-related cross-sectional ASD and TD group mean trajectories and were not able to quantify individual-level deviation. In the future, the quantification of an individual's deviation from normative trajectories will be informative [77]. Using longitudinal data which we are currently collecting (R01MH132218), the GAM framework can extend to longitudinal within-individual analyses to parse deviations during aging across adulthood in autism.

Conclusion

Resting-state functional connectivity changes nonlinearly with age in diverse curvatures across typically developing functional networks. Connectivity in ASD also follows nonlinear cross-sectional age-related trajectories that can be both divergent or congruent with typical development. Generalized additive models are an

advanced statistical modeling tool to enable flexible non-linear aging models while simultaneously parsing group differences that appear during brain developmental and maturational periods in autistic individuals.

Abbreviations

ASD	Autism spectrum disorder
TD	Typically developing
rs-fMRI	Resting-state functional magnetic resonance imaging
GAM	Generalized additive model; FDR: false-discovery rate; DMN: default mode network
CEN	Central executive network
MSP	Medial superior parietal
DAN	Dorsal attention network
VAN	Ventral attention network
SMN	Somatomotor network
SMNa	Somatomotor association network

Supplementary Information

The online version contains supplementary material available at <https://doi.org/10.1186/s13229-025-00657-1>.

Supplementary Material 1

Acknowledgements

Research reported in this publication was supported by the National Institute of Mental Health of the National Institutes of Health under Award Number R01MH132218. The content is solely the responsibility of the authors and does not necessarily represent the official views of the National Institutes of Health.

Author contributions

DAF, MBDP, and JBK developed the concept. DAF wrote the main manuscript text. DAF and JBK performed all analyses. DAF prepared all figures. MBDP, ALA, BAZ, and JEL edited the manuscript. All authors reviewed the manuscript.

Funding

DAF was supported by the NSF GRFP under grant number 2139322, JBK was supported by NIA grant number K01AG075166, and all authors received support under NIMH grant number R01MH132218.

Data availability

The datasets analyzed during the current study are available in the ABIDE repository, https://fcon_1000.projects.nitrc.org/indi/abide/.

Declarations

Ethics approval and consent to participate

Ethics approval was acquired by each individual site within the ABIDE repository.

Consent for publication

Not applicable.

Competing interests

The authors declare no competing interests.

Author details

¹Department of Biomedical Engineering, University of Utah, Salt Lake City, UT 84112, USA

²Department of Radiology & Imaging Sciences, University of Utah, Salt Lake City, UT 84112, USA

³Waisman Center, University of Wisconsin-Madison, Madison, WI 53706, USA

⁴Department of Psychiatry, University of Wisconsin-Madison, Madison, WI 53706, USA

⁵Department of Medical Physics, University of Wisconsin-Madison, Madison, WI 53706, USA

⁶Department of Pediatrics, Neurology, and Neuroscience, University of Florida, Gainesville, FL 32611, USA

Received: 28 November 2024 / Accepted: 22 March 2025

Published online: 15 April 2025

References

1. Lau WKW, Leung MK, Lau BWM. Resting-state abnormalities in autism spectrum disorders: a meta-analysis. *Sci Rep*. 2019;9(1):3892.
2. Rane P, Cochran D, Hodge SM, Haselgrove C, Kennedy D, Frazier JA. Connectivity in autism: a review of MRI connectivity studies. *Harv Rev Psychiatry*. 2015;23(4):223–44.
3. Hull JV, Dokovna LB, Jacokes ZJ, Torgerson CM, Irimia A, Van Horn JD. Resting-State functional connectivity in autism spectrum disorders: A review. *Front Psychiatry*. 2017;7:205.
4. Guo Z, Tang X, Xiao S, Yan H, Sun S, Yang Z, et al. Systematic review and meta-analysis: multimodal functional and anatomical neural alterations in autism spectrum disorder. *Mol Autism*. 2024;15(1):16.
5. Ilioska I, Oldehinkel M, Llera A, Chopra S, Looden T, Chauvin R, et al. Connectome-wide mega-analysis reveals robust patterns of atypical functional connectivity in autism. *Biol Psychiatry*. 2023;94(1):29–39.
6. Holiga S, Hipp JF, Chatham CH, Garces P, Spooren W, D'Ardhu XL, et al. Patients with autism spectrum disorders display reproducible functional connectivity alterations. *Sci Transl Med*. 2019;11(481):eaat9223.
7. King JB, Prigge MBD, King CK, Morgan J, Weathersby F, Fox JC, et al. Generalizability and reproducibility of functional connectivity in autism. *Mol Autism*. 2019;10:27.
8. Nomi JS, Uddin LQ. Developmental changes in large-scale network connectivity in autism. *NeuroImage: Clin*. 2015;7:732–41.
9. Padmanabhan A, Lynn A, Foran W, Luna B, O'Hearn K. Age related changes in striatal resting state functional connectivity in autism. *Front Hum Neurosci*. 2013;7:814.
10. Haghghat H, Mirzarezaee M, Araabi BN, Khadem A. Functional networks abnormalities in autism spectrum disorder: age-related hypo and hyper connectivity. *Brain Topogr*. 2021;34(3):306–22.
11. Long Z, Duan X, Mantini D, Chen H. Alteration of functional connectivity in autism spectrum disorder: effect of age and anatomical distance. *Sci Rep*. 2016;6(1):26527.
12. Fan F, Liao X, Lei T, Zhao T, Xia M, Men W, et al. Development of the default-mode network during childhood and adolescence: A longitudinal resting-state fMRI study. *NeuroImage*. 2021;226:117581.
13. Gracia-Tabuenca Z, Moreno MB, Barrios FA, Alcauter S. Development of the brain functional connectome follows puberty-dependent nonlinear trajectories. *NeuroImage*. 2021;229:117769.
14. López-Vicente M, Agcaoglu O, Pérez-Crespo L, Estévez-López F, Heredia-Genestar JM, Mulder RH, et al. Developmental changes in dynamic functional connectivity from childhood into adolescence. *Front Syst Neurosci*. 2021;15:724805.
15. Ma ZH, Lu B, Li X, Mei T, Guo YQ, Yang L, et al. Atypicalities in the developmental trajectory of cortico-striatal functional connectivity in autism spectrum disorder. *Autism*. 2022;26(5):1108–22.
16. Sanders AFP, Harms MP, Kandala S, Marek S, Somerville LH, Bookheimer SY, et al. Age-related differences in resting-state functional connectivity from childhood to adolescence. *Cereb Cortex*. 2023;33(11):6928–42.
17. Sun L, Zhao T, Liang X, Xia M, Li Q, Liao X et al. Functional connectome through the human life span. *BioRxiv*. 2024;2023.09.12.557193.
18. Edde M, Leroux G, Altena E, Chanraud S. Functional brain connectivity changes across the human life span: from fetal development to old age. *J Neurosci Res*. 2021;99(1):236–62.
19. Luo N, Sui J, Abrol A, Lin D, Chen J, Vergara VM, et al. Age-related structural and functional variations in 5,967 individuals across the adult lifespan. *Hum Brain Mapp*. 2019;41(7):1725–37.
20. Jacobs HIL, Müller-Ehrenberg L, Priovoulos N, Roebroeck A. Curvilinear locus coeruleus functional connectivity trajectories over the adult lifespan: a 7T MRI study. *Neurobiol Aging*. 2018;69:167–76.
21. Wang Q, Qi L, He C, Feng H, Xie C. Age- and gender-related dispersion of brain networks across the lifespan. *GeroScience*. 2023;46(1):1303–18.
22. Hastie T, Tibshirani R. Generalized additive models. *Stat Sci*. 1986;1(3):297–310.

23. Rubinstein YD, Hastie T. 1997. Discriminative vs informative learning. In Proceedings of the Third International Conference on Knowledge Discovery and Data Mining (KDD'97). AAAI Press, 49–53.
24. Wood SN, Augustin NH. GAMs with integrated model selection using penalized regression splines and applications to environmental modeling. *Ecol Model*. 2002;157(2):157–77.
25. Alaerts K, Nayar K, Kelly C, Raithe J, Milham MP, Di Martino A. Age-related changes in intrinsic function of the superior Temporal sulcus in autism spectrum disorders. *Soc Cognit Affect Neurosci*. 2015;10(10):1413–23.
26. Henry TR, Dichter GS, Gates K. Age and gender effects on intrinsic connectivity in autism using functional integration and segregation. *Biol Psychiatry: Cogn Neurosci Neuroimaging*. 2018;3(5):414–22.
27. Di Martino A, Yan CG, Li Q, Denio E, Castellanos FX, Alaerts K, et al. The autism brain imaging data exchange: towards Large-Scale evaluation of the intrinsic brain architecture in autism. *Mol Psychiatry*. 2014;19(6):659–67.
28. Di Martino A, O'Connor D, Chen B, Alaerts K, Anderson JS, Assaf M, et al. Enhancing studies of the connectome in autism using the autism brain imaging data exchange II. *Sci Data*. 2017;4:170010.
29. Napolitano A, Schiavi S, La Rosa P, Rossi-Espagnet MC, Petrillo S, Bottino F et al. Sex differences in autism spectrum disorder: diagnostic, neurobiological, and behavioral features. *Front Psychiatry*. 2022 May 13.
30. Reuter M, Rosas HD, Fischl B. Highly accurate inverse consistent registration: a robust approach. *NeuroImage*. 2010;53(4):1181–96.
31. Segonne F, Dale AM, Busa E, Glessner M, Salat D, Hahn HK, et al. A hybrid approach to the skull stripping problem in MRI. *NeuroImage*. 2004;22(3):1060–75.
32. Fischl B, Salat DH, Busa E, Albert M, Dieterich M, Haselgrove C, et al. Whole brain segmentation: automated labeling of neuroanatomical structures in the human brain. *Neuron*. 2002;33(3):341–55.
33. Fischl B, van der Kouwe A, Destrieux C, Halgren E, Segonne F, Salat DH, et al. Automatically parcellating the human cerebral cortex. *Cereb Cortex*. 2004;14(1):11–22.
34. Sled JG, Zijdenbos AP, Evans AC. A nonparametric method for automatic correction of intensity nonuniformity in MRI data. *IEEE Trans Med Imaging*. 1998;17(1):87–97.
35. Fischl B, Liu A, Dale AM. Automated manifold surgery: constructing geometrically accurate and topologically correct models of the human cerebral cortex. *IEEE Trans Med Imaging*. 2001;20(1):70–80.
36. Segonne F, Pacheco J, Fischl B. Geometrically accurate topology-correction of cortical surfaces using nonseparating loops. *IEEE Trans Med Imaging*. 2007;26(4):518–29.
37. Dale AM, Fischl B, Sereno MI. Cortical surface-based analysis. I. Segmentation and surface reconstruction. *NeuroImage*. 1999;9(2):179–94.
38. Dale AM, Sereno MI. Improved localization of cortical activity by combining EEG and MEG with MRI cortical surface reconstruction: A linear approach. *J Cogn Neurosci*. 1993;5:162–76.
39. Fischl B, Dale AM. Measuring the thickness of the human cerebral cortex from magnetic resonance images. *Proc Natl Acad Sci USA*. 2000;97(20):11050–5.
40. Anderson JS, Druzgal TJ, Lopez-Larson M, Jeong E, Desai K, Yurgelun-Todd D. Network anticorrelations, global regression, and phase-shifted soft tissue correction. *Hum Brain Mapp*. 2010;32(6):919–34.
41. 1, Murphy K, Fox MD. Towards a consensus regarding global signal regression for resting state functional connectivity MRI. *NeuroImage*. 2017;154:169–73.
42. Power JD, Barnes KA, Snyder AZ, Schlaggar BL, Petersen SE. Spurious but systematic correlations in functional connectivity MRI networks arise from subject motion. *NeuroImage*. 2012;59(3):2142.
43. Thomas Yeo BT, Krienen FM, Sepulcre J, Sabuncu MR, Lashkari D, Hollinshead M, et al. The organization of the human cerebral cortex estimated by intrinsic functional connectivity. *J Neurophysiol*. 2011;106(3):1125–65.
44. Pomponio R, Erus G, Habes M, Doshi J, Srinivasan D, Mamourian E, et al. Harmonization of large MRI datasets for the analysis of brain imaging patterns throughout the lifespan. *NeuroImage*. 2020;208:116450.
45. Fortin JP, Parker D, Tunç B, Watanabe T, Elliott MA, Ruparel K, et al. Harmonization of multi-site diffusion tensor imaging data. *NeuroImage*. 2017;161:149–70.
46. Hu F, Chen AA, Horng H, Bashyam V, Davatzikos C, Alexander-Bloch A, et al. Image harmonization: A review of statistical and deep learning methods for removing batch effects and evaluation metrics for effective harmonization. *NeuroImage*. 2023;274:120125.
47. Wood SN. Thin plate regression splines. *J Royal Stat Society: Ser B (Statistical Methodology)*. 2003;65(1):95–114.
48. R Core Team. (2023). R: a language and environment for statistical computing. R Foundation for Statistical Computing, Vienna, Austria. <https://www.R-project.org/>
49. Wickham H. (2016). ggplot2: Elegant graphics for data analysis. Springer-Verlag New York. ISBN 978-3-319-24277-4. <https://ggplot2.tidyverse.org>
50. Wood SN. Generalized additive models: an introduction with R, Second Edition. 2nd ed. New York: Chapman and Hall/CRC; 2017. P. 496.
51. Coretta S. Tidygam: tidy prediction and plotting of generalized additive models. 2023. Available from: <https://cran.r-project.org/web/packages/tidygam/index.html>
52. Moghimi P, Dang AT, Do Q, Netoff TI, Lim KO, Atluri G. Evaluation of functional MRI-based human brain parcellation: a review. *J Neurophysiol*. 2022;128(1):197–217.
53. Bryce NV, Flournoy JC, Guassi Moreira JF, Rosen ML, Sambook KA, Mair P, et al. Brain parcellation selection: an overlooked decision point with meaningful effects on individual differences in resting-state functional connectivity. *NeuroImage*. 2021;243:118487.
54. Zhou Z, Srinivasan D, Li H, Abdulkadir A, Shou H, Davatzikos C, et al. Harmonization of multi-site functional connectivity measures in tangent space improves brain age prediction. *Proc SPIE Int Soc Opt Eng*. 2022;12036:1203608.
55. Yu M, Linn KA, Cook PA, Phillips ML, McInnis M, Fava M, et al. Statistical harmonization corrects site effects in functional connectivity measurements from multi-site fMRI data. *Hum Brain Mapp*. 2018;39(11):4213–27.
56. Prigge MBD, Lange N, Bigler ED, King JB, Dean DC, Adluru N, et al. A 16-year study of longitudinal volumetric brain development in males with autism. *NeuroImage*. 2021;236:118067.
57. Van Rooij D, Anagnostou E, Arango C, Auzias G, Behrmann M, Busatto GF, et al. Cortical and subcortical brain morphometry differences between patients with autism spectrum disorder and healthy individuals across the lifespan: results from the ENIGMA ASD working group. *AJP*. 2018;175(4):359–69.
58. Nunes AS, Vakorin VA, Kozhemiako N, Peatfield N, Ribary U, Doesburg SM. Atypical age-related changes in cortical thickness in autism spectrum disorder. *Sci Rep*. 2020;10(1):11067.
59. Zhou R, Sun C, Sun M, Ruan Y, Li W, Gao X. Altered intra- and inter-network connectivity in autism spectrum disorder. *Aging*. 2024;16(11):10004.
60. Lynch CJ, Uddin LQ, Supekar K, Khouzam A, Phillips J, Menon V. Default mode network in childhood autism: posteromedial cortex heterogeneity and relationship with social deficits. *Biol Psychiatry*. 2013;74(3):212–9.
61. Buckner RL. The brain's default network: origins and implications for the study of psychosis. *Dialog Clin Neurosci*. 2013;15(3):351.
62. Greicius MD, Krasnow B, Reiss AL, Menon V. Functional connectivity in the resting brain: a network analysis of the default mode hypothesis. *Proceedings of the National Academy of Sciences*. 2003;100(1):253–8.
63. Padmanabhan A, Lynch CJ, Schaer M, Menon V. The default mode network in autism. *Biol Psychiatry Cogn Neurosci Neuroimaging*. 2017;2(6):476.
64. Menon V. 20 Years of the default mode network: A review and synthesis. *Neuron*. 2023;111(16):2469–87.
65. Bhat AN. Motor impairment increases in children with autism spectrum disorder as a function of social communication, cognitive and functional impairment, repetitive behavior severity, and comorbid diagnoses: a SPARK study report. *Autism Research: Official J Int Soc Autism Res*. 2020;14(1):202.
66. Marco EJ, Hinkley LBN, Hill SS, Nagarajan SS. Sensory processing in autism: a review of neurophysiologic findings. *Pediatr Res*. 2011;69(5 Pt 2):48R.
67. Wigham S, Rodgers J, South M, McConachie H, Freeston M. The interplay between sensory processing abnormalities, intolerance of uncertainty, anxiety and restricted and repetitive behaviours in autism spectrum disorder. *J Autism Dev Disord*. 2015;45(4):943–52.
68. Bethlehem Ra, Seidlitz I, White J, Vogel SR, Anderson JW, Adamson KM. Brain charts for the human lifespan. *Nature*. 2022;604(7906):525–33.
69. Bozek J, Griffanti L, Lau S, Jenkinson M. Normative models for neuroimaging markers: impact of model selection, sample size and evaluation criteria. *NeuroImage*. 2023;268:119864.
70. Ge R, Yu Y, Qi YX, Fan Y, nan, Chen S, Gao C, et al. Normative modelling of brain morphometry across the lifespan with centilebrain: algorithm benchmarking and model optimisation. *Lancet Digit Health*. 2024;6(3):e211–21.
71. Bedford SA, Lai MC, Lombardo MV, Chakrabarti B, Ruigrok A, Suckling J et al. Brain-Charting autism and Attention-Deficit/Hyperactivity disorder reveals distinct and overlapping neurobiology. *Biol Psychiatry*. 2024 Aug 14.
72. Stasinopoulos DM, Rigby RA. Generalized additive models for location scale and shape (GAMLSS) in R. *J Stat Soft*. 2007;23(7):1–46.

73. Alaerts K, Swinnen SP, Wenderoth N. Sex differences in autism: a resting-state fMRI investigation of functional brain connectivity in males and females. *Soc Cogn Affect Neurosci*. 2016;11(6):1002–16.
74. Tavares V, Fernandes LA, Antunes M, Ferreira H, Prata D. Sex differences in functional connectivity between resting state brain networks in autism spectrum disorder. *J Autism Dev Disord*. 2022;52(7):3088–101.
75. Sonido M, Arnold S, Higgins J, Hwang YJ. Autism in later life: what is known and what is needed? *Curr Dev Disord Rep*. 2020;7(2):69–77.
76. Mason D, Stewart GR, Capp SJ, Happé F. Older age autism research: a rapidly growing field, but still a long way to go. *Autism Adulthood*. 2022;4(2):164–72.
77. Gardner M, Shinohara RT, Bethlehem RAI, Romero-Garcia R, Warrier V, Dorschmidt L et al. ComBatLS: A location- and scale-preserving method for multi-site image harmonization. *BioRxiv*. 2024;2024.06.21.599875.

Publisher's note

Springer Nature remains neutral with regard to jurisdictional claims in published maps and institutional affiliations.